Geophysical Research Letters

RESEARCH LETTER
10.1029/2023GL106413

Deglacial Carbon Escape From the Northern Rim of the Southern Ocean

N. E. Umling[1], E. Sikes[2], P. Rafter[3], N. F. Goodkin[1], and J. R. Southon[3]

[1]Department of Earth and Planetary Sciences, American Museum of Natural History, New York, NY, USA, [2]Department of Marine and Coastal Sciences, Rutgers University, New Brunswick, NJ, USA, [3]Department of Earth System Sciences, University of California, Irvine, CA, USA

Key Points:

- Indian Ocean Antarctic Intermediate Water was a pathway for ventilation of a deglacial carbon reservoir
- Latitudinal shifts in the Southern Ocean fronts contributed to glacial carbon storage and deglacial ventilation
- Intermediate waters of the Southern Indian Ocean were more than 2,000 years older in the deglaciation than the glacial and Holocene

Supporting Information:

Supporting Information may be found in the online version of this article.

Correspondence to:

N. E. Umling,
numling@amnh.org

Citation:

Umling, N. E., Sikes, E., Rafter, P., Goodkin, N. F., & Southon, J. R. (2024). Deglacial carbon escape from the northern rim of the Southern Ocean. *Geophysical Research Letters*, *51*, e2023GL106413. https://doi.org/10.1029/2023GL106413

Received 18 OCT 2023
Accepted 8 FEB 2024

Abstract The Southern Ocean regulates atmospheric CO_2 and Earth's climate as a critical region for air-sea gas exchange, delicately poised between being a CO_2 source and sink. Here, we estimate how long a water mass has remained isolated from the atmosphere and utilize $^{14}C/^{12}C$ ratios ($\Delta^{14}C$) to trace the pathway and escape route of carbon sequestered in the deep ocean through the mixed layer to the atmosphere. The position of our core at the northern margin of the Southern Indian Ocean, tracks latitudinal shifts of the Southern Ocean frontal zones across the deglaciation. Our results suggest an expanded glacial Antarctic region trapped CO_2, whereas deglacial expansion of the subantarctic permitted ventilation of the trapped CO_2, contributing to a rapid atmospheric CO_2 rise. We identify frontal positions as a key factor balancing CO_2 outgassing versus sequestration in a region currently responsible for nearly half of global ocean CO_2 uptake.

Plain Language Summary The Southern Ocean is a key region for the inhalation and exhalation of carbon dioxide, responsible for absorbing nearly half of the total amount of atmospheric c taken up by the modern global ocean. Today, regions of communication between the deep ocean and atmosphere are bounded by oceanographic fronts. During cold glacial periods, when sea ice cover expanded in the Southern Ocean, these regions were shifted northward. Our data shows that this northward movement pinched together the fronts in the Southern Indian Ocean, restricting glacial ocean-atmosphere gas exchange, allowing CO_2 to accumulate in the deep ocean. We find that at the end of the glaciation, the fronts returned southward and expanded, allowing transfer of the stored CO_2 into intermediate and surface waters before escaping to the atmosphere. This trapping and releasing mechanism driven by frontal shifts is important for understanding how changes in Southern Ocean dynamics can affect the ability of the oceans to take up the additional atmospheric CO_2 produced from human activities.

1. Introduction

Over at least the last ~800,000 years (Bereiter et al., 2015), rising temperatures have been linked to increasing atmospheric CO_2 concentrations, and global climate feedbacks that flip the switch between glacial and interglacial climate states. Cold climate conditions during glacial maximums are associated with a transfer of CO_2 from the atmosphere into the deep ocean resulting from altered global ocean overturning circulation (Broecker & Barker, 2007; Curry & Oppo, 2005; McManus et al., 2004) and more efficient biological transfer of carbon from the surface to deep ocean (Kohfeld, 2005). The transition to the warmer climate conditions of interglaciations rapidly releases this stored carbon to the surface ocean as ocean circulation returns to modern configuration (Anderson et al., 2009; Broecker & Barker, 2007). There is an abundance of evidence for a respired CO_2 reservoir in the glacial deep ocean (Anderson et al., 2019; Curry & Oppo, 2005; Hoogakker et al., 2018; Skinner et al., 2017) and the timing of the deglacial increase in atmospheric CO_2 is well-constrained (Marcott et al., 2014). However, evidence for the dynamic interactions that transfer carbon stored in the ocean to the atmosphere is lacking. The Indian Ocean sector of the Southern Ocean (Figure 1) has an abundance of bathymetric features that enhance eddy mixing, fostering air sea exchange within the Southern Ocean's Antarctic Circumpolar Current (ACC; Brady et al., 2021; Rintoul, 2018) making it a crucial location for examining millennial scale changes in deep ocean uptake and release of CO_2.

In today's Southern Ocean, atmosphere-ocean CO_2 exchange is associated with seasonal CO_2 outgassing through wind-driven upwelling of old, carbon-rich deep waters (Gray et al., 2018) that have accumulated respired CO_2 as they remained out of contact with the atmosphere on their journey along the global ocean conveyor belt (Talley

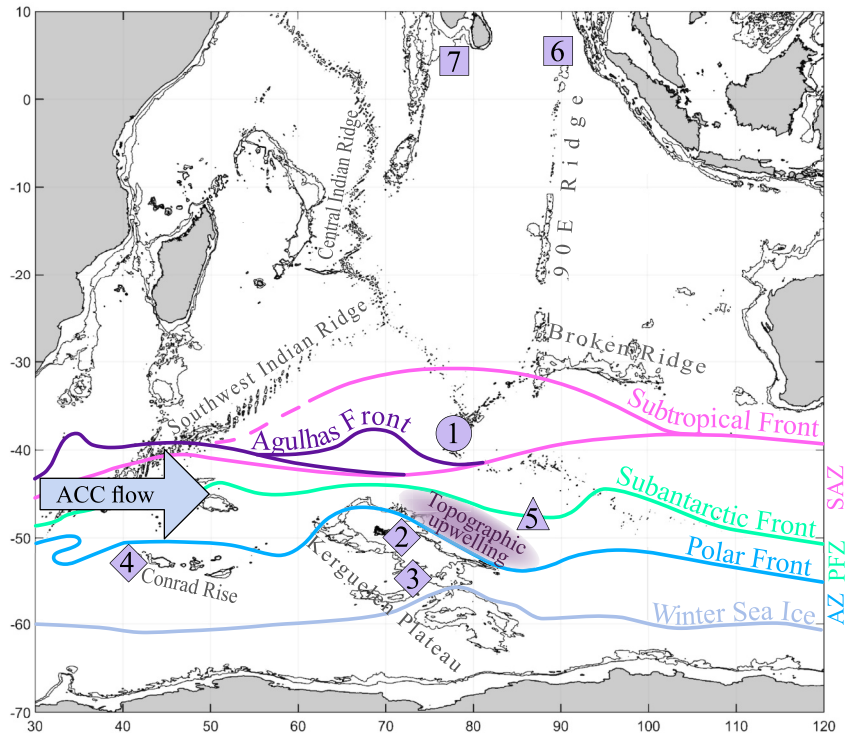

Figure 1. TT1811-50GGC is located in the subtropical zone of the southern Indian Ocean (1 = TT1811-50GGC, 1,116 m, 38.344°S, 77.715°E) between the volcanic hot spot islands Île Amsterdam and Île St. Paul. Nearby published records from the Kerguelen Plateau (2 = PS69/912-3&4, 567 m; 3 = PS69/907-20, 2,253 m; Ronge et al., 2020), Conrad Rise (4 = PS2606-6, 2,545 m; Ronge et al., 2020), and Australian-Antarctic Basin (5 = MD12-3396CQ, 3,615 m; Gottschalk et al., 2020), span the Antarctic frontal zone and the northern Indian Ocean (6 = SS-172/4040, 2,788 m; 7 = SS152-3828, 3,166 m; Bharti et al., 2022). Frontal definitions from Belkin and Gordon (1996).

et al., 2011). The deep-water radiocarbon content ($\Delta^{14}C$) of dissolved CO_2 decays as a water mass remains out of contact with the atmosphere. In the southern Indian Ocean, southward-flowing Indian Deep Water (IDW) delivers aged, ^{14}C-depleted, CO_2-rich, waters supplying Upper Circumpolar Deep Water (UCDW), which upwells to the north of the Polar Front (PF) and to the south of the Antarctic Subantarctic Front (SAF) in the Polar Frontal Zone (PFZ; Key et al., 2004; Paterne et al., 2019). Wind stress nudges this water northward toward the Subantarctic Zone (SAZ) where it becomes more buoyant through warming and freshening while it ventilates CO_2 to the atmosphere and acquires atmospheric ^{14}C (Key et al., 2004; Talley et al., 2011). These dynamics create the shallow water masses of the Southern Ocean overturning circulation; Antarctic Intermediate Water (AAIW) and Subantarctic Mode Water (SAMW; Figure 2; Talley et al., 2011), which trace the ^{14}C balance of carbon sequestration and carbon release as influenced by surface ocean equilibration with the atmosphere and the input of deep, ^{14}C-depleted waters to the mixed layer of the surface ocean.

Here, we provide a record of changes in the relative water mass age of surface and AAIW waters based on the $\Delta^{14}C$ of paired planktic (*Globigerina inflata*; lower mixed layer-dwelling) and mixed benthic foraminifera from a marine sediment core (TT1811-50GGC; 38.344°S, 77.715°E; 1,116 m, Figure 1) collected between Île Amsterdam and Île St. Paul, just north of the northern boundary of the Southern Ocean (defined by the modern Subtropical Front; STF; Talley et al., 2011). This site sits at the depth of modern AAIW (Figure 2) and is ideally positioned to monitor climate-driven shifts in the Southern Ocean frontal system and the latitudinal expansion and contraction of the Southern Ocean for the last ~40,000 years (Figure 1).

2. Materials and Methods

Marine sediment core TT1811-50GGC was collected by the R.V. Thomas G. Thompson in late-2018 from 1,116 m water depth along the southeast Indian Ridge between Île Amsterdam and Île St. Paul (38.344°S, 77.715°E). Seventy-five sample depths were analyzed for planktic and benthic radiocarbon content (Figure S1 in Supporting

10.1029/2023GL106413

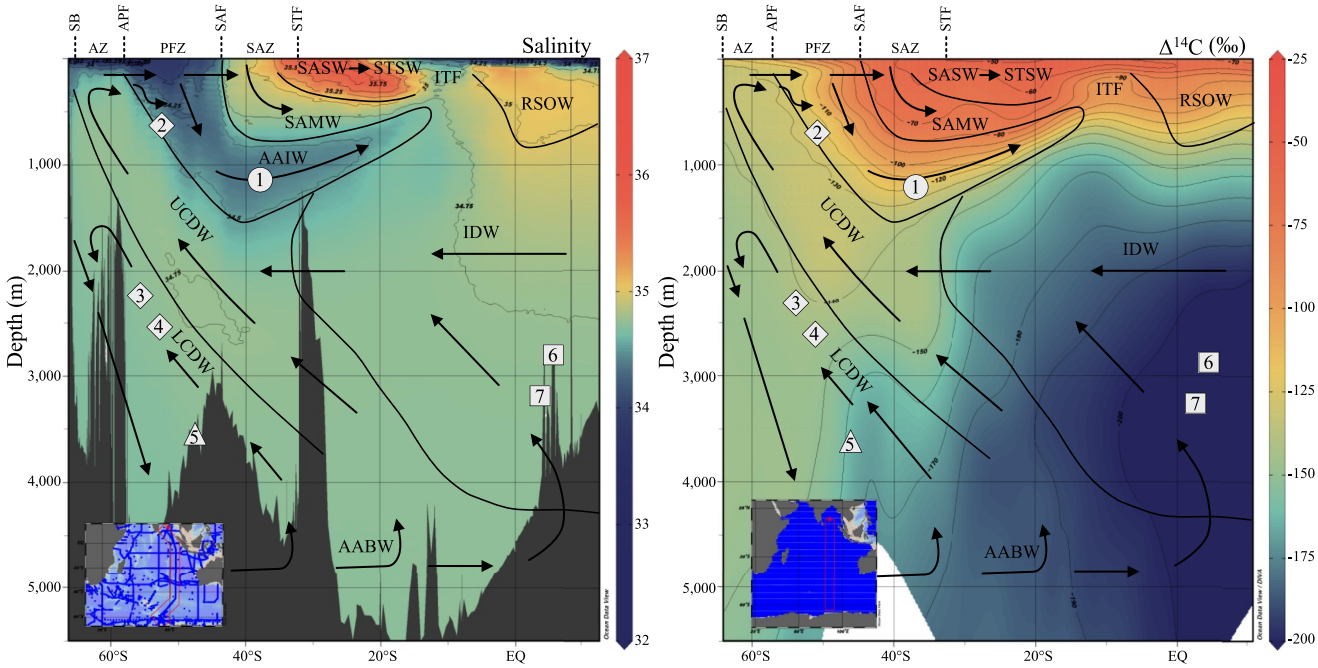

Figure 2. Our Île St. Paul core (1 = TT1811-50GGC) falls within AAIW, shown in east Indian Ocean transects (inset) of salinity[56] (left; Olsen et al., 2020) and natural (pre-bomb) $\Delta^{14}C$ (right; Key et al., 2004) with water masses overlain according to the definitions of Talley et al. (2011). Paleo-radiocarbon studies from the Kerguelen Plateau (2 = PS69/912-3&4; 3 = PS69/907-2; Ronge et al., 2020), Conrad Rise (4 = PS2606-6; Ronge et al., 2020), Australian-Antarctic Basin (5 = MD12-3396CQ; Gottschalk et al., 2020), and the northern Indian Ocean (6 = SS-172/4040; 7 = SS152-3828; Bharti et al., 2022). Sections generated using Ocean Data View (Schlitzer, 2015) with color palette by P. Rafter (https://prafter.com/color/). SASW, Subantarctic Surface Water; STSW, Subtropical Surface Water; ITF, Indonesian Throughflow; SAMW, Subantarctic Mode Water; RSOW, Red Sea Overflow Water; IDW, Indian Deep Water; UCDW, Upper Circumpolar Deep Water; LCDW, Lower Circumpolar Deep Water.

Information S1). The lower mixed layer dwelling planktic foraminifera *Globorotalia inflata* was selected for radiocarbon analyses as it is persistent species throughout the core and is abundant during the austral spring (King & Howard, 2005). In this region, the spring mixed layer is deep (200–500 m on average) and poorly stratified (Sallée et al., 2006). Mixed benthic for radiocarbon analyses were selected with care taken to exclude benthic species with deep (>2 cm) infaunal depth habitats (*Globobulimina*, *Chilostomella*, etc.; McCorkle et al., 1990), porcelaneous textures (*Pyrgo*; Magana et al., 2010), and agglutinated compositions. Prior to analysis of radiocarbon content at the Keck Carbon Cycle Accelerator Mass Spectrometer Facility at the University of California, Irvine, 10% of each sample was leached using weak HCl to remove authigenic carbonates and graphitized per Santos et al. (2007).

The oxygen isotopic composition ($\delta^{18}O$) of the mixed-layer planktic foraminifera species *Globigerina bulloides*, the thermocline dwelling species *Globorotalia truncatulanoides*, and the benthic foraminifera *Cibicidoides lobatulus* were analyzed on a Finnigan MAT-253 Plus Isotope Ratio Mass Spectrometer (IRMS) with a Kiel IV device at the City of New York's Advanced Science Research Center (ASRC) and at the University of Florida Light Stable Isotope Mass Spectrometry Laboratory in the Department of Geological Sciences with a Kiel III carbonate preparation device coupled with a Finnigan-Mat 252 isotope ratio mass spectrometer. Long term precision of repeated $\delta^{18}O$ measurement of the NBS-19 standard across the measurement period was ±0.05‰ VPDB and ±0.06‰, respectively.

The age model for TT1811-50GGC was constrained by identifying changes persistent in both the oxygen isotope record of *G. bulloides* and *G. truncatulanoides* that were coeval with Antarctic temperature and $\delta^{18}O$ events in the EPICA (European Project for Ice Coring in Antarctica) Dome C (EDC; Buizert et al., 2015; Buizert et al., 2021; Lorius et al., 1979) and Dome Fuji (Fujita et al., 2015; Kawamura et al., 2007; Watanabe et al., 2003) ice cores synchronized to the layer counted West Antarctic Ice Sheet Divide ice core (WD2014; Figure S2 in Supporting Information S1; Buizert et al., 2018). The rapid thermal equilibration of circum-Antarctic surface waters and Antarctic air temperatures is known to be transmitted to the EPICA Dome C ice core through an atmospheric

connection. This understanding is the basis for the widespread use of tying $\delta^{18}O$ and Sea Surface Temperature (SST) records to Antarctic ice cores (i.e., Gottschalk et al., 2020; Rose et al., 2010; Skinner et al., 2010). To address any possible local salinity effect on the planktic $\delta^{18}O$, tie-points were verified with co-occurring changes in thermocline (*G. truncatulanoides*) and benthic (*C. lobatulus*) $\delta^{18}O$ (Figure S2 in Supporting Information S1). The slight variations in the timing of events in the $\delta^{18}O$ records fall within our estimated age model and reservoir age error.

Initial reservoir ages were determined by correcting the *G. inflata* ^{14}C-ages to calendar ages using the pre-industrial reservoir age estimated for the Kerguelen Islands ($\Delta R = 442 \pm 101$; Paterne et al., 2019) from the marine reservoir correction database (Reimer & Reimer, 2001) with an error of ± 101 added to allow for the documented preindustrial range of ^{14}C variability (Paterne et al., 2019). Using the initial alignment of the ^{14}C-calibrated ages, the match between surface ocean (*G. bulloides*) and thermocline (*G. truncatulanoides*) $\delta^{18}O$ with Holocene temperature and $\delta^{18}O$ EDC events was reassessed. Surface ocean $\delta^{18}O$ values that showed an EDC match within the Holocene reservoir age error window were then aligned to the EDC matches. As the early Holocene portion of the core has less variability in Antarctic temperature and $\delta^{18}O$, the ^{14}C-calibrated ages were used for age control (Figure S2; Table S1 in Supporting Information S1).

Primary concerns when analyzing past oceanic radiocarbon variability are the development of a rigorous age model and sedimentary or diagenetic influences on radiocarbon age. These concerns are often related. The presence of ash layers or terrestrial sourced plant material can provide an independent constraint on sediment age (Sikes et al., 2000; Zhao et al., 2018). Distinct thin ash layers and dispersed ash are present in TT1811-50GGC as shallow as 60 cm (Figure S3 in Supporting Information S1), but these ashes have not been linked to a dated terrestrial event and may be submarine in origin. However, the changes in core color associated with the presence of ash and/or changes in deposition provide useful sedimentary contacts that can confirm minimal mixing. Bioturbation and mixing can homogenize sedimentary contacts or result in a mottled rather than sharp basal contact. The presence of sharp basal contacts in 50GGC suggests that mixing and bioturbation was relatively minimal in the deglacial and glacial portions of the core (Figure S3 in Supporting Information S1). Also, changes in sediment color and sedimentation rate are roughly contemporaneous with changes in benthic assemblage and *Cibicidoides lobatulus* oxygen isotopic composition (Figure S3 in Supporting Information S1) suggesting a primarily climatological rather than sedimentary control.

The final chronology was calculated using the Bayesian analysis age modeling program Bacon (version 2.5.7; Blaauw & Christen, 2011; Figure S4 in Supporting Information S1) in the open-source statistical software R (version 4.2.1; R Core Team, 2022). Uncertainty in the EDC WD2014 age model was propagated with a matching error before reconstructing the Bayesian accumulation histories. The median offset between the foraminifera ages and the atmosphere (Reservoir ages) were estimated using the Reservoir Age offset package (ResAge; Soulet, 2015; Figure S5 in Supporting Information S1) with the Southern Hemisphere SHCal20 reference record (Hogg et al., 2020) in R (legacy version 3.3.1; R Core Team, 2022). Measured $\Delta^{14}C$ values were corrected for ^{14}C decay that has occurred in the time after the forams died and were initially deposited to estimate the initial radiocarbon content ($\Delta^{14}C_0$) of the sample (Adkins & Boyle, 1997).

3. Glacial

The Holocene $\Delta^{14}C$ in our core reflects the modern surface ocean $\Delta^{14}C$ equilibration dynamics (Figure 3b), with mean Holocene planktic reservoir ages of ~940 years (Figure 3d) mirroring the modern reservoir ages documented in bivalves from Kerguelen Island (~920 years; Paterne et al., 2019). The modern latitudinal surface ocean ^{14}C gradient tracks the progressive CO_2 release (Key et al., 2004) and this pattern allows us to use planktic ^{14}C to track the intensity of past equilibration, while our benthic ^{14}C traces the reservoir age of the upwelled UCDW, which appears to have been ~6,000 years in the LGM. However, latitudinal shifts in Southern Ocean frontal boundaries have been documented to have occurred in this region (Bard & Rickaby, 2009; Civel-Mazens et al., 2021; Howard & Prell, 1992; Kohfeld et al., 2013; Moros et al., 2021; Shetye et al., 2014; Thöle et al., 2022), complicating interpretations.

We can tackle the issue of climate related north-south shifts in Southern Ocean fronts by leveraging the AAIW-to-surface vertical ^{14}C gradient (Figure 2) in our core to better reconstruct the depth and latitude of the northward flowing tongue of AAIW through time in the context of regional records of latitudinal SST gradients, faunal distributions, and productivity. A shoaling and/or poleward shift of the AAIW tongue relative to our site would

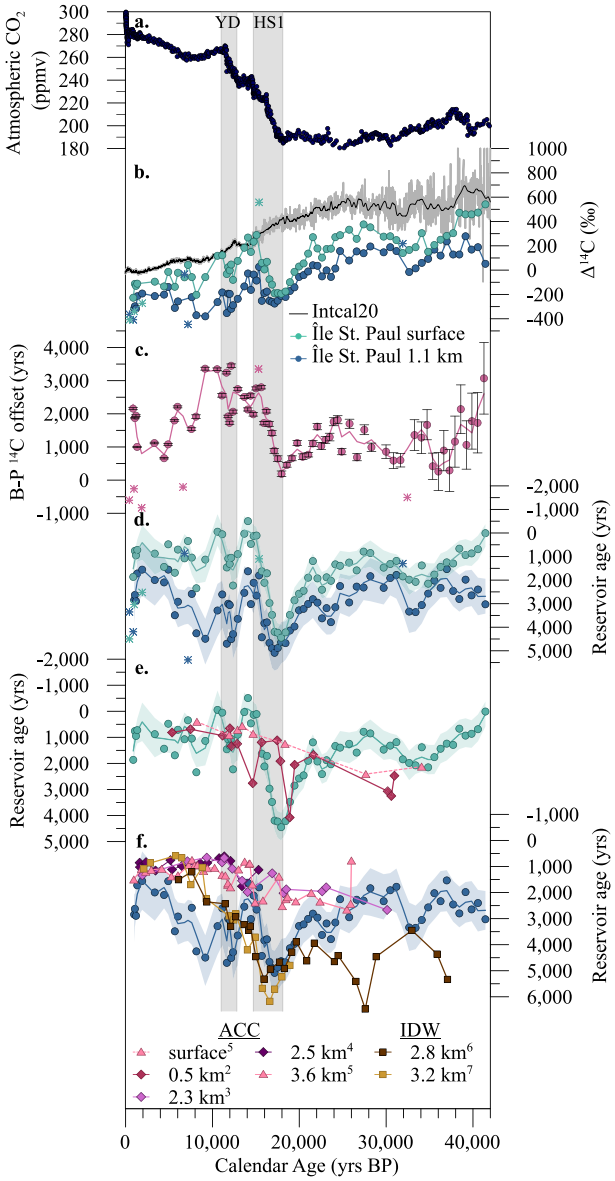

Figure 3. (a) The deglacial increase in atmospheric CO_2 (Bereiter et al., 2015; Marcott et al., 2014) is mirrored by changes in the (b) atmospheric radiocarbon content ($\Delta^{14}C$; Reimer et al., 2020) and the $\Delta^{14}C$ of Southern Indian Ocean surface waters and Antarctic Intermediate Water (AAIW). (c) The AAIW ^{14}C offset from the surface ocean (B-P ^{14}C offset) and the (d) reservoir ages (^{14}C offset from the contemporaneous atmosphere) of Île St. Paul AAIW and surface waters are variable across the deglaciation. The reservoir error windows (see methods) are shown as green (*G. inflata*) and blue (mixed benthics) shaded regions. Regional comparison of (e) surface and shallow subsurface records along with (f) deep ocean records from the Kerguelen Plateau (2 = PS69/912-3&4; 3 = PS69/907-2; Ronge et al., 2020) Conrad Rise (4 = PS2606-6; Ronge et al., 2020), Australian-Antarctic Basin (5 = MD12-3396CQ; Gottschalk et al., 2020), and the northern Indian Ocean (6 = SS-172/4040; 7 = SS152-3828; Bharti et al., 2022). YD, Younger Dryas; HS1, Heinrich Stadial 1.

increase the vertical ^{14}C gradient by moving the locus of the gradient minimum (Figure S6 in Supporting Information S1), resulting in a larger offset between the benthic and planktic ^{14}C (B-P offset). A B-P offset approaching zero indicates a deepening of AAIW convection and/or a equatorward shift of the Southern Ocean fronts would place the zone of AAIW convection toward our site. A moderate B-P gradient of ~1,170 years in the Holocene reflects the modern location of TT1811-50GGC within the mid-point of AAIW (Figure 2). Our B-P results prior to the LGM (from ~30 to 22 ka) mirror the late Holocene AAIW-to-surface vertical ocean ^{14}C configuration, with similar surface ocean and AAIW reservoir ages (Figure 3d). This suggests that the ventilation of shallow water masses prior to the LGM were not largely different from today and places UCDW upwelling firmly south of our core location from ~30 to 22 ka.

These results contrast with published results from a nearby site at 3,615 m water depth that sits in Lower Circumpolar Deep Water (LCDW) and indicates that from 30 to 22 ka LCDW was ~1,000 years older than present (Figure 3f; Gottschalk et al., 2020; Ronge et al., 2020). Today, LCDW is formed as the ACC mixes with southward flowing North Atlantic Deep Water and northward flowing Antarctic Bottom Water (AABW) that forms along the continental margin of Antarctica, subducts, and moves northward at abyssal depths (Figure 2; Talley et al., 2011). Older LCDW during the ~7 ka before the LGM likely stemmed from isolation of LCDW from the atmosphere while at the surface as a result of expanded winter sea ice (Ferrari et al., 2014; Gersonde et al., 2005; WAIS Divide Project Members, 2015), allowing these waters to retain an aged ^{14}C value. Recirculation of this older LCDW as AABW northward would account for the aging of IDW and UCDW prior to the LGM (Figures 3e and 3f; Bharti et al., 2022; Ronge et al., 2020).

Paired SST and biological productivity evidence from South of Africa indicate the STF had reached its northernmost position prior to 30 ka and remained there relatively constantly from 30 to 18 ka (Bard & Rickaby, 2009) whereas evidence from cores near our site indicate that the SAF and PF continued to move northwards from 30 ka into the LGM (Civel-Mazens et al., 2021). This paints a picture of an expanded PFZ and a progressively narrowing SAZ. Today, deep winter mixing of SAMW in the SAZ reventilates recently subducted waters (Koch-Larrouy et al., 2010), but a tightened belt of SAZ would have contributed to a reconfigured Southern Ocean that may have not aligned with the Westerly winds, an arrangement that would have restricted CO_2 outgassing (Russell et al., 2006; Toggweiler et al., 2006). We hypothesize this was instrumental to keeping atmospheric CO_2 low (Marcott et al., 2014) during the LGM (Figures 3a and 4a).

4. LGM

The most dramatic signal in our record is a ~3,000 years increase in surface and AAIW reservoir ages during the LGM (~22–18 ka; Figure 3d). Such old reservoir ages can only be the result of very old deep waters coming to the surface (Figure 4b). Equally old reservoir ages to the south and west of our site were recorded in UCDW during the LGM (Figure 3e; Ronge et al., 2020), while the presence of similarly aged IDW in the equatorial Indian Ocean at mid-depths (Bharti et al., 2022) point to IDW as the source of the old, ^{14}C-depleted waters present in UCDW at these sites. Decreasing B-P ^{14}C offsets between AAIW and surface waters (Figure 3c) and an equatorward shift in the Southern Ocean fronts suggested by other studies (Bard & Rickaby, 2009; Civel-Mazens et al., 2021; Kohfeld et al., 2013; Li et al., 2010; Moros et al., 2021; Thöle et al., 2022) across this glaciation, place our core in the SAZ region of AAIW

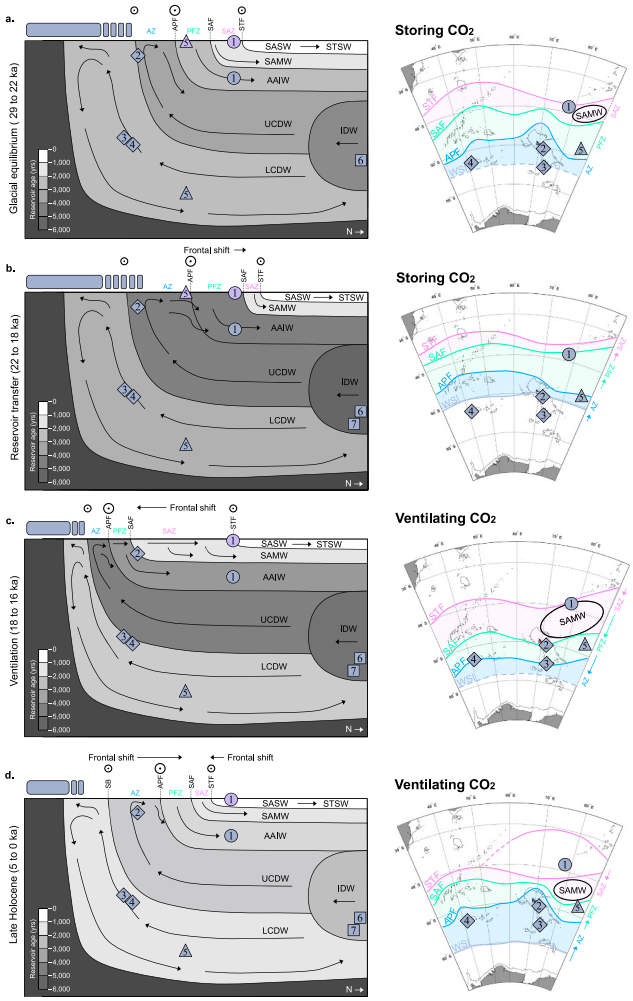

Figure 4. Generalized latitudinal depth-transect showing the ventilation scheme (left) and predicted Southern Ocean frontal locations (right) during the (a) glacial (~29–22 ka), (b) late Last Glacial Maximum (LGM; ~20 to 18 ka), (c) Heinrich Stadial 1 (HS1; ~18 to 15 ka), and (d) modern Southern Indian Ocean. Each *x*-axis tick-mark in the middle panel represents 1,000 years. Paleo-radiocarbon studies for Île St. Paul (1 = TT1811-50GGC), Kerguelen Plateau (2 = PS69/912-3&4; 3 = PS69/907-2; Ronge et al., 2020), Conrad Rise (4 = PS2606-6; Ronge et al., 2020), Australian-Antarctic Basin (5 = MD12-3396CQ; Gottschalk et al., 2020), and the northern Indian Ocean (6 = SS-172/4040; 7 = SS152-3828; Bharti et al., 2022) are indicated in blue for benthic records and purple for planktic records.

convection. The continued shift of the PF and SAF to their most northerly positions (Bard & Rickaby, 2009; Civel-Mazens et al., 2021; Kohfeld et al., 2013; Li et al., 2010; Moros et al., 2021; Thöle et al., 2022) increasingly narrowed the SAZ and AZ, which appears to have caused upwelled UCDW to subduct as AAIW without allowing degassing or resetting the ^{14}C-depleted signature. We hypothesize this propagated an aged signal into the interior of the Indian Ocean where it may have recirculated as IDW of increasing age (Figure 4b). Deep water masses exchange through diapycnal mixing in which small scale turbulence mixes oppositely traveling water masses, entraining AAIW and AABW into IDW along density surfaces (de Lavergne et al., 2017). In the glacial Indian Ocean, this would have increased the reservoir age in IDW that was subsequently upwelled as UCDW and transferred back to AAIW as Earth descended into the LGM (22-18 ka; Figure 3e). The lack of a change in atmospheric Δ^{14}C composition supports our interpretation that old CO_2 was recirculated into the mid depths of the Indian Ocean (Figure 3b) through the LGM, increasing the age of this regional reservoir until the start of Heinrich Stadial 1 (~15–18 ka). Unchanged LCDW ventilation (Figure 3f; Gottschalk et al., 2020; Ronge et al., 2020) suggests these waters were mixing with AABW that was more ventilated than UCDW. Because CO_2 equilibrates more rapidly with the atmosphere than the isotopes of carbon, this could have resulted in decoupling of radiocarbon signatures and gas exchange. However, relatively stable LGM atmospheric CO_2 levels suggest that this was likely not a significant source of CO_2 to the atmosphere at this time. Model simulations have projected that reduced deep ocean ventilation was linked to expanded sea ice along with equatorward shifted Westerlies and Southern Ocean fronts in the LGM (Chen & Wang, 2021; Ferrari et al., 2014; Mandal et al., 2021; Menviel et al., 2015; Russell et al., 2006; Toggweiler et al., 2006). These new data are the first to clarify that the individual fronts did not move in sync or in parallel and identifies that the narrowing of the SAZ in the Indian Ocean was a significant process sequestering CO_2.

5. Deglaciation

Notably, the maximum offset to the atmosphere in both surface (~4,400 years) and AAIW (~5,000 years) waters (Figure 3d) occurred at the transition from the LGM to Heinrich Stadial 1 (~18 ka) at our site (Figure 3d). This is coeval with a minimum in B-P ^{14}C (~200 years; Figure 3c), suggesting the locus of UCDW upwelling and AAIW formation was positioned close to our core site. The presence of very old IDW at that time in the northern Indian Ocean (Figure 3f; Bharti et al., 2022) and the appearance of aged UCDW briefly to the south of our site, at Kerguelen (~4,075 years; Figure 3e; Ronge et al., 2020), indicates these conditions marked the apex of the CO_2 sequestration event in the LGM.

Coinciding with Heinrich Stadial 1, the reservoir ages of AAIW and surface waters off Île St. Paul rapidly decreased, documenting the rapid, progressive loss of aged CO_2 from the SAZ in the Indian Ocean. A coeval decrease in IDW reservoir ages in the northern Indian Ocean (Figure 3f; Bharti et al., 2022) documents the flushing of old CO_2 from mid-depth waters (Figure 4c). During HS1, the Île St. Paul B-P ^{14}C offset increased (Figure 3c), which we interpret as a poleward shift of the SAF to the south of Île St. Paul and/or a shoaling of the depth of the AAIW tongue. Regionally, there is evidence for SAF retreat southwards (Moros et al., 2021) and warming sea surface temperatures (Gottschalk et al., 2020; Shukla et al., 2021; Thöle et al., 2022) across the southern Indian Ocean at this time, which we infer widened the SAZ and allowed the slow (decadal) equilibration of ^{14}C during the escape of CO_2 from the surface ocean. A widening SAZ appears to have opened a valve from the deep ocean to the atmosphere while deep winter mixing progressively ventilated AAIW and SAMW at our site. A

^{14}C-depleted signal is recorded briefly in shallow subsurface waters at Kerguelen (~0.5 km water depth; Figure 3f; Ronge et al., 2020), verifying this effect was regional.

It is important to point out that the ^{14}C-depleted signal in both surface and AAIW at our site indicates this is the location of upwelling and likely not the site where full equilibration and ventilation occurred at this time. Mechanistically, bottom topography serves to steer the ACC and instigate upwelling in the Southern Ocean (Rintoul, 2018). The main flow of the ACC in the Indian Ocean is squeezed between the Kerguelen Plateau and the plateau where Île St. Paul sits, prompting topographic upwelling in the shadow of Kerguelen (Brady et al., 2021) and activating SAMW formation and ventilation (Figure 1) as waters in the SAZ are swept along in the ACC (Koch-Larrouy et al., 2010; Rintoul, 2018). Models show that today, water rises to the surface in the topographic upwelling domain created by the Kerguelen Plateau (Brady et al., 2021) and ventilates as they move eastward to the South Tasman Rise before sinking as SAMW (Koch-Larrouy et al., 2010). Deep winter mixing in the SAZ ventilates these waters as they transit across the Southern Ocean (Rintoul, 2018) and may be responsible for the progressive loss of the depleted ^{14}C signal in SAMW and AAIW seen off New Zealand (Rose et al., 2010) and the Chilean Margin (Siani et al., 2013) during the LGM and deglaciation. The verification of the SAZ as a locus of deglacial CO_2 degassing has been demonstrated previously by boron isotope records of surface ocean pH from the SAZ in the Pacific and South Atlantic (Martínez-Botí et al., 2015; Moy et al., 2019; Shao et al., 2019), which document the presence of CO_2-rich waters during the first half of the deglaciation.

Our results imply that a northern migration of Southern Ocean fronts during and prior to the LGM (~30–18 ka) may have altered the intersection of the ACC with the Kerguelen Plateau and generally reduced topographic driven turbulent mixing, thereby impacting overturning circulation by dampening deep-water mixing, upwelling, and the associated air sea exchange in this region (Ferrari et al., 2014). We suggest southward frontal migrations during the deglaciation (Anderson et al., 2009; Bostock et al., 2015; Moros et al., 2021; Sikes et al., 2009), would have re-invigorated Kerguelen-driven upwelling. Evidence suggests that while the SAF and PF began their trek southward at ~22 ka, the STF remained northward until ~18.5 ka (Moros et al., 2021; Sikes et al., 2009), contributing to an expanded SAZ and broad region allowing ventilation and SAMW formation (Koch-Larrouy et al., 2010). We hypothesize the combination of re-invigorated topographic-driven upwelling and a widened SAZ served to super charge ventilation in a broad swath of the Southern Ocean at the start of the deglaciation (Figure 4c).

At the onset of the Antarctic Cold Reversal/Bølling Allerød (~15 ka), the Île St. Paul benthic (AAIW) reservoir ages at our site had returned to late glacial values. In contrast, surface waters ages overshot their Holocene mean, reaching near-atmospheric values (<500 years; Figure 3d). The Antarctic Cold Reversal (~15–13 ka; Figure 3d) was characterized by cooler, surface temperatures (Civel-Mazens et al., 2021; Moros et al., 2021; Sikes et al., 2009; WAIS Divide Project Members, 2015), expanded sea ice (Ferrari et al., 2014; Gersonde et al., 2005), and northward movement of Southern Ocean fronts (Civel-Mazens et al., 2021; Moros et al., 2021; Sikes et al., 2009). It is also associated with a pause in atmospheric CO_2 rise (Figure 3a; Marcott et al., 2014) and decreasing Δ^{14}C (Figure 3b; Reimer et al., 2020). It is uncertain why our surface ages were very young, although well-ventilated mixed layer waters during the Antarctic Cold Reversal could have been achieved by an over invigorated AMOC (Barker et al., 2010). Similar to the early glaciation, the B-P offset at our site indicates there was a hiatus in ventilation of the deep carbon reservoir through AAIW. We suggest that much like during glaciation, the frontal positions in the Indian Ocean contributed to this hiatus and the pause in CO_2 rise (Marcott et al., 2014).

During the millennial period immediately following the Antarctic Cold Reversal (Younger Dryas; ~13 to 11.7 ka), surface ocean reservoir ages at Île St. Paul site increase to Holocene-like values (Figure 3d), consistent with reservoir ages documented in UCDW-bathed cores to the south, off the Kerguelen plateau (Figure 3e; Ronge et al., 2020). However, at our site, Younger Dryas AAIW reservoir ages increased to values almost equal to the peak recorded at the glacial/HS1 transition and remained elevated until ~8 ka (Figure 3d). This is echoed in the persistent old ages recorded in northern Indian Ocean IDW cores (Figure 3f; Bharti et al., 2022). Additionally, the B-P ^{14}C offset at our site remained elevated and increased to a maximum B-P offset during the early Holocene (Figure 3c) suggesting a shoaled and/or southward shift in the locus of AAIW convection. The fact that our AAIW values were similar to or greater than IDW in the northern Indian Ocean (Figure 3f; Bharti et al., 2022) suggests that there was continued transfer of the IDW ^{14}C-depleted signal southward to our site allowing its subsequent release from the Southern Ocean during the second half of the deglaciation and into the early Holocene. This

contrasts with the first half of the deglaciation when our results suggest CO_2 equilibration was farther downstream in the ACC. These results substantiate the involvement of Southern Ocean dynamics in the return of trapped CO_2 to the atmosphere throughout the deglaciation.

6. Conclusions

Our radiocarbon records emphasize the interplay of SAZ expansion and topographic mixing for enhancing CO_2 ventilation from the deep ocean to the atmosphere at the end of the last ice age. This work highlights the role that shifting fronts played in driving SAMW formation and the past modulation of oceanic CO_2 uptake and release from the Southern Ocean. Modern hydrographic studies are documenting signs that the modern ACC has been both strengthening (Freeman et al., 2016; Shi et al., 2021) and migrating poleward (Lee et al., 2023; Yamazaki et al., 2021) as our climate warms. Much like the deglaciation, the attendant thickening and strengthening of SAMW formation that has been documented in the modern Southern Indian Ocean (Lu et al., 2021) may indicate expansion of the SAZ that could foretell a Southern Ocean shift from a CO_2 sink to a CO_2 source as the globe continues to warm.

Conflict of Interest

The authors declare no conflicts of interest relevant to this study.

Data Availability Statement

The benthic and planktonic foraminiferal oxygen isotope and radiocarbon data generated in this study are available from the National Centers for Environmental Information (Umling et al., 2024). The statistical analysis was carried out using the open-source statistical software R (R Core Team, 2022), the ResAge (Soulet, 2015), and rbacon (Blaauw & Christen, 2011) packages.

Acknowledgments
This research was supported by the National Science Foundation Grants OCE159080 and OCE1940962 to ELS and OCE 2002630 to NEU and NFG. The data sets generated during this study have been archived at the National Centers for Environmental Information.

References

Adkins, J. F., & Boyle, E. A. (1997). Changing atmospheric $\Delta^{14}C$ and the record of deep water paleoventilation ages. *Paleoceanography*, *12*(3), 337–344. https://doi.org/10.1029/97PA00379

Anderson, R. F., Ali, S., Bradtmiller, L. I., Nielsen, S. H. H., Fleisher, M. Q., Anderson, B. E., & Burckle, L. H. (2009). Wind-driven upwelling in the Southern Ocean and the deglacial rise in atmospheric CO_2. *Science*, *323*(5920), 1443–1448. https://doi.org/10.1126/science.1167441

Anderson, R. F., Sachs, J. P., Fleisher, M. Q., Allen, K. A., Yu, J., Koutavas, A., & Jaccard, S. L. (2019). Deep-sea oxygen depletion and Ocean Carbon sequestration during the last ice age. *Global Biogeochemical Cycles*, *33*(3), 301–317. https://doi.org/10.1029/2018GB006049

Bard, E., & Rickaby, R. E. M. (2009). Migration of the subtropical front as a modulator of glacial climate. *Nature*, *460*(7253), 380–383. https://doi.org/10.1038/nature08189

Barker, S., Knorr, G., Vautravers, M. J., Diz, P., & Skinner, L. C. (2010). Extreme deepening of the Atlantic overturning circulation during deglaciation. *Nature Geoscience*, *3*(8), 567–571. https://doi.org/10.1038/ngeo921

Belkin, I. M., & Gordon, A. L. (1996). Southern Ocean fronts from the Greenwich meridian to Tasmania. *Journal of Geophysical Research*, *101*(C2), 3675–3696. https://doi.org/10.1029/95JC02750

Bereiter, B., Eggleston, S., Schmitt, J., Nehrbass-Ahles, C., Stocker, T. F., Fischer, H., et al. (2015). Revision of the EPICA Dome C CO_2 record from 800 to 600 kyr before present: Analytical bias in the EDC CO_2 record. *Geophysical Research Letters*, *42*(2), 542–549. https://doi.org/10.1002/2014GL061957

Bharti, N., Bhushan, R., Skinner, L., Muruganantham, M., Jena, P. S., Dabhi, A., & Shivam, A. (2022). Evidence of poorly ventilated deep Central Indian Ocean during the last glaciation. *Earth and Planetary Science Letters*, *582*, 117438. https://doi.org/10.1016/j.epsl.2022.117438

Blaauw, M., & Christen, J. A. (2011). Flexible paleoclimate age-depth models using an autoregressive gamma process (version 2.5.7). Software. *Bayesian Analysis*, *6*, 457–474. https://doi.org/10.1214/ba/1339616472

Bostock, H. C., Hayward, B. W., Neil, H. L., Sabaa, A. T., & Scott, G. H. (2015). Changes in the position of the Subtropical Front south of New Zealand since the last glacial period. *Paleoceanography*, *30*(7), 824–844. https://doi.org/10.1002/2014PA002652

Brady, R. X., Maltrud, M. E., Wolfram, P. J., Drake, H. F., & Lovenduski, N. S. (2021). The influence of ocean topography on the upwelling of carbon in the Southern Ocean. *Geophysical Research Letters*, *48*(19). https://doi.org/10.1029/2021GL095088

Broecker, W., & Barker, S. (2007). A 190‰ drop in atmosphere's $\Delta^{14}C$ during the "Mystery Interval" (17.5 to 14.5 kyr). *Earth and Planetary Science Letters*, *256*(1–2), 90–99. https://doi.org/10.1016/j.epsl.2007.01.015

Buizert, C., Adrian, B., Ahn, J., Albert, M., Alley, R. B., Baggenstos, D., et al. (2015). Precise interpolar phasing of abrupt climate change during the last ice age. *Nature*, *520*(7549), 661–665. https://doi.org/10.1038/nature14401

Buizert, C., Fudge, T. J., Roberts, W. H. G., Steig, E. J., Sherriff-Tadano, S., Ritz, C., et al. (2021). Antarctic surface temperature and elevation during the last glacial maximum. *Science*, *372*(6546), 1097–1101. https://doi.org/10.1126/science.abd2897

Buizert, C., Sigl, M., Severi, M., Markle, B. R., Wettstein, J. J., McConnell, J. R., et al. (2018). Abrupt ice-age shifts in southern westerly winds and Antarctic climate forced from the north. *Nature*, *563*(7733), 681–685. https://doi.org/10.1038/s41586-018-0727-5

Chen, C., & Wang, G. (2021). Simulated Southern Ocean upwelling at the last glacial maximum and early deglaciation: The role of eddy-induced overturning circulation. *Geophysical Research Letters*, *48*(9). https://doi.org/10.1029/2021GL092880

Civel-Mazens, M., Crosta, X., Cortese, G., Michel, E., Mazaud, A., Ther, O., et al. (2021). Antarctic polar front migrations in the Kerguelen Plateau region, Southern Ocean, over the past 360 kyrs. *Global and Planetary Change*, *202*, 103526. https://doi.org/10.1016/j.gloplacha.2021.103526

Curry, W. B., & Oppo, D. W. (2005). Glacial water mass geometry and the distribution of $\delta^{13}C$ of ΣCO_2 in the western Atlantic Ocean. *Paleoceanography*, *20*(1). https://doi.org/10.1029/2004PA001021

De Lavergne, C., Madec, G., Roquet, F., Holmes, R. M., & McDougall, T. J. (2017). Abyssal Ocean overturning shaped by seafloor distribution. *Nature*, *551*(7679), 181–186. https://doi.org/10.1038/nature24472

Ferrari, R., Jansen, M. F., Adkins, J. F., Burke, A., Stewart, A. L., & Thompson, A. F. (2014). Antarctic sea ice control on ocean circulation in present and glacial climates. *Proceedings of the National Academy of Sciences*, *111*(24), 8753–8758. https://doi.org/10.1073/pnas.1323922111

Freeman, N. M., Lovenduski, N. S., & Gent, P. R. (2016). Temporal variability in the Antarctic polar front (2002-2014). *Journal of Geophysical Research: Oceans*, *121*(10), 7263–7276. https://doi.org/10.1002/2016JC012145

Fujita, S., Parrenin, F., Severi, M., Motoyama, H., & Wolff, E. W. (2015). Volcanic synchronization of Dome Fuji and Dome C Antarctic deep ice cores over the past 216 kyr. *Climate of the Past*, *11*(10), 1395–1416. https://doi.org/10.5194/cp-11-1395-2015

Gersonde, R., Crosta, X., Abelmann, A., & Armand, L. (2005). Sea-Surface temperature and Sea ice distribution of the Southern Ocean at the EPILOG last glacial maximum—A circum-Antarctic view based on siliceous microfossil records. *Quaternary Science Reviews*, *24*(7–9), 869–896. https://doi.org/10.1016/j.quascirev.2004.07.015

Gottschalk, J., Michel, E., Thöle, L. M., Studer, A. S., Hasenfratz, A. P., Schmid, N., et al. (2020). Glacial heterogeneity in Southern Ocean carbon storage abated by fast South Indian deglacial carbon release. *Nature Communications*, *11*(1), 6192. https://doi.org/10.1038/s41467-020-20034-1

Gray, A. R., Johnson, K. S., Bushinsky, S. M., Riser, S. C., Russell, J. L., Talley, L. D., et al. (2018). Autonomous biogeochemical floats detect significant carbon dioxide outgassing in the high-latitude Southern Ocean. *Geophysical Research Letters*, *45*(17), 9049–9057. https://doi.org/10.1029/2018GL078013

Hogg, A. G., Heaton, T. J., Hua, Q., Palmer, J. G., Turney, C. S., Southon, J., et al. (2020). SHCal20 southern hemisphere calibration, 0–55,000 years cal BP. *Radiocarbon*, *62*(4), 759–778. https://doi.org/10.1017/RDC.2020.59

Hoogakker, B. A. A., Lu, Z., Umling, N., Jones, L., Zhou, X., Rickaby, R. E. M., et al. (2018). Glacial expansion of oxygen-depleted seawater in the eastern tropical Pacific. *Nature*, *562*(7727), 410–413. https://doi.org/10.1038/s41586-018-0589-x

Howard, W. R., & Prell, W. L. (1992). Late quaternary surface circulation of the southern Indian ocean and its relationship to orbital variations. *Paleoceanography*, *7*(1), 79–117. https://doi.org/10.1029/91PA02994

Kawamura, K., Parrenin, F., Lisiecki, L., Uemura, R., Vimeux, F., Severinghaus, J. P., et al. (2007). Northern Hemisphere forcing of climatic cycles in Antarctica over the past 360,000 years. *Nature*, *448*(7156), 912–916. https://doi.org/10.1038/nature06015

Key, R. M., Kozyr, A., Sabine, C. L., Lee, K., Wanninkhof, R., Bullister, J. L., et al. (2004). A global ocean carbon climatology: Results from global data analysis Project (GLODAP). *Global Biogeochemical Cycles*, *18*(4). https://doi.org/10.1029/2004GB002247

King, A. L., & Howard, W. R. (2005). $\delta^{18}O$ seasonality of planktonic foraminifera from Southern Ocean sediment traps: Latitudinal gradients and implications for paleoclimate reconstructions. *Marine Micropaleontology*, *56*(1–2), 1–24. https://doi.org/10.1016/j.marmicro.2005.02.008

Koch-Larrouy, A., Morrow, R., Penduff, T., & Juza, M. (2010). Origin and mechanism of subantarctic mode water formation and transformation in the southern Indian ocean. *Ocean Dynamics*, *60*(3), 563–583. https://doi.org/10.1007/s10236-010-0276-4

Kohfeld, K. E., Graham, R. M., De Boer, A. M., Sime, L. C., Wolff, E. W., Le Quéré, C., & Bopp, L. (2013). Southern Hemisphere westerly wind changes during the last glacial maximum: Paleo-data synthesis. *Quaternary Science Reviews*, *68*, 76–95. https://doi.org/10.1016/j.quascirev.2013.01.017

Kohfeld, K. E., Quéré, C. L., Harrison, S. P., & Anderson, R. F. (2005). Role of marine biology in glacial-interglacial CO_2 cycles. *Science*, *308*(5718), 74–78. https://doi.org/10.1126/science.1105375

Lee, S.-K., Lumpkin, R., Gomez, F., Yeager, S., Lopez, H., Takglis, F., et al. (2023). Human-induced changes in the global meridional overturning circulation are emerging from the Southern Ocean. *Communications Earth & Environment*, *4*(1), 69. https://doi.org/10.1038/s43247-023-00727-3

Li, W., Wang, R., Xiang, F., Ding, X., & Zhao, M. (2010). Sea surface temperature and subtropical front movement in the South Tasman Sea during the last 800 ka. *Chinese Science Bulletin*, *55*(29), 3338–3344. https://doi.org/10.1007/s11434-010-4074-7

Lorius, C., Merlivat, L., Jouzel, J., & Pourchet, M. (1979). A 30,000-yr isotope climatic record from Antarctic ice. *Nature*, *280*(5724), 644–648. https://doi.org/10.1038/280644a0

Lu, Y., Liu, Q., & Xie, S.-P. (2021). Covariability of subantarctic mode water and the southern Branch of the subtropical Indian ocean countercurrent in argo observations. *Journal of Ocean University of China*, *20*(6), 1316–1324. https://doi.org/10.1007/s11802-021-4677-4

Magana, A. L., Southon, J. R., Kennett, J. P., Roark, E. B., Sarnthein, M., & Stott, L. D. (2010). Resolving the cause of large differences between deglacial benthic foraminifera radiocarbon measurements in Santa Barbara Basin. *Paleoceanography*, *25*(4), PA4102. https://doi.org/10.1029/2010PA002011

Mandal, G., Lee, S.-Y., & Yu, J.-Y. (2021). The roles of wind and Sea ice in driving the deglacial change in the Southern Ocean upwelling: A modeling study. *Sustainability*, *13*(1), 353. https://doi.org/10.3390/su13010353

Marcott, S. A., Bauska, T. K., Buizert, C., Steig, E. J., Rosen, J. L., Cuffey, K. M., et al. (2014). Centennial-scale changes in the global carbon cycle during the last deglaciation. *Nature*, *514*(7524), 616–619. https://doi.org/10.1038/nature13799

Martínez-Botí, M. A., Marino, G., Foster, G. L., Ziveri, P., Henehan, M. J., Rae, J. W. B., et al. (2015). Boron isotope evidence for oceanic carbon dioxide leakage during the last deglaciation. *Nature*, *518*(7538), 219–222. https://doi.org/10.1038/nature14155

McCorkle, D. C., Keigwin, L. D., Corliss, B. H., & Emerson, S. R. (1990). The influence of microhabitats on the carbon isotopic composition of deep-sea benthic foraminifera. *Paleoceanography*, *5*(2), 161–185. https://doi.org/10.1029/PA005i002p00161

McManus, J. F., Francois, R., Gherardi, J.-M., Keigwin, L. D., & Brown-Leger, S. (2004). Collapse and rapid resumption of Atlantic meridional circulation linked to deglacial climate changes. *Nature*, *428*(6985), 834–837. https://doi.org/10.1038/nature02494

Menviel, L., Spence, P., Golledge, N., & England, M. H. (2015). Southern Ocean overturning role in modulating high southern latitude climate and atmospheric CO2 on millennial timescales. *Nova Acta Leopoldina NF*, *121*(408), 159–166.

Moros, M., De Deckker, P., Perner, K., Ninnemann, U. S., Wacker, L., Telford, R., et al. (2021). Hydrographic shifts south of Australia over the last deglaciation and possible interhemispheric linkages. *Quaternary Research*, *102*, 130–141. https://doi.org/10.1017/qua.2021.12

Moy, A. D., Palmer, M. R., Howard, W. R., Bijma, J., Cooper, M. J., Calvo, E., et al. (2019). Varied contribution of the Southern Ocean to deglacial atmospheric CO_2 rise. *Nature Geoscience*, *12*(12), 1006–1011. https://doi.org/10.1038/s41561-019-0473-9

Olsen, A., Lange, N., Key, R. M., Tanhua, T., Bittig, H. C., Kozyr, A., et al. (2020). An updated version of the global interior ocean biogeochemical data product, GLODAPv2.2020. *Earth System Science Data*, *12*(4), 3653–3678. https://doi.org/10.5194/essd-12-3653-2020

Paterne, M., Michel, E., & Héros, V. (2019). Variability of marine 14C reservoir ages in the Southern Ocean highlighting circulation changes between 1910 and 1950. *Earth and Planetary Science Letters*, *511*, 99–104. https://doi.org/10.1016/j.epsl.2019.01.029

R Core Team. (2022). *A language and environment for statistical computing (version 4.2.1and legacy version 3.3.1). Software*. R Foundation for Statistical Computing. Retrieved from https://www.R-project.org/

Reimer, P. J., Austin, W. E. N., Bard, E., Bayliss, A., Blackwell, P. G., Bronk Ramsey, C., et al. (2020). The IntCal20 northern Hemisphere radiocarbon age calibration curve (0–55 cal kBP). *Radiocarbon*, *62*(4), 725–757. https://doi.org/10.1017/RDC.2020.41

Reimer, P. J., & Reimer, R. W. (2001). A marine reservoir correction database and on-line interface. *Radiocarbon*, *43*(2A), 461–463. https://doi.org/10.1017/S0033822200038339

Rintoul, S. R. (2018). The global influence of localized dynamics in the Southern Ocean. *Nature*, *558*(7709), 209–218. https://doi.org/10.1038/s41586-018-0182-3

Ronge, T. A., Prange, M., Mollenhauer, G., Ellinghausen, M., Kuhn, G., & Tiedemann, R. (2020). Radiocarbon evidence for the contribution of the southern Indian ocean to the evolution of atmospheric CO_2 over the last 32,000 years. *Paleoceanography and Paleoclimatology*, *35*(3). https://doi.org/10.1029/2019PA003733

Rose, K. A., Sikes, E. L., Guilderson, T. P., Shane, P., Hill, T. M., Zahn, R., & Spero, H. J. (2010). Upper-ocean-to-atmosphere radiocarbon offsets imply fast deglacial carbon dioxide release. *Nature*, *466*(7310), 1093–1097. https://doi.org/10.1038/nature09288

Russell, J. L., Dixon, K. W., Gnanadesikan, A., Stouffer, R. J., & Toggweiler, J. R. (2006). The southern Hemisphere westerlies in a warming World: Propping open the door to the deep ocean. *Journal of Climate*, *19*(24), 6382–6390. https://doi.org/10.1175/JCLI3984.1

Sallée, J.-B., Wienders, N., Speer, K., & Morrow, R. (2006). Formation of subantarctic mode water in the southeastern Indian Ocean. *Ocean Dynamics*, *56*(5–6), 525–542. https://doi.org/10.1007/s10236-005-0054-x

Santos, G. M., Moore, R. B., Southon, J. R., Griffin, S., Hinger, E., & Zhang, D. (2007). AMS 14C sample preparation at the KCCAMS/UCI facility: Status report and performance of small samples. *Radiocarbon*, *49*(2), 255–269. https://doi.org/10.1017/S0033822200042181

Schlitzer, R. (2015). Ocean data view. Retrieved from https://odv.awi.de/

Shao, J., Stott, L. D., Gray, W. R., Greenop, R., Pecher, I., Neil, H. L., et al. (2019). Atmosphere-Ocean CO_2 exchange across the last deglaciation from the boron isotope proxy. *Paleoceanography and Paleoclimatology*, *34*(10), 1650–1670. https://doi.org/10.1029/2018PA003498

Shetye, S. S., Mohan, R., & Nair, A. (2014). Latitudinal shifts in the polar front in Indian sector of the Southern Ocean: Evidences from silicoflagellate assemblage. *Geosciences Journal*, *18*(2), 241–246. https://doi.org/10.1007/s12303-013-0061-8

Shi, J.-R., Talley, L. D., Xie, S.-P., Peng, Q., & Liu, W. (2021). Ocean warming and accelerating Southern Ocean zonal flow. *Nature Climate Change*, *11*(12), 1090–1097. https://doi.org/10.1038/s41558-021-01212-5

Shukla, S. K., Crosta, X., & Ikehara, M. (2021). Sea surface temperatures in the Indian sub-Antarctic Southern Ocean for the last four interglacial periods. *Geophysical Research Letters*, *48*(8). https://doi.org/10.1029/2020GL090994

Siani, G., Michel, E., De Pol-Holz, R., DeVries, T., Lamy, F., Carel, M., et al. (2013). Carbon isotope records reveal precise timing of enhanced Southern Ocean upwelling during the last deglaciation. *Nature Communications*, *4*(1), 2758. https://doi.org/10.1038/ncomms3758

Sikes, E. L., Howard, W. R., Samson, C. R., Mahan, T. S., Robertson, L. G., & Volkman, J. K. (2009). Southern Ocean seasonal temperature and subtropical front movement on the South Tasman rise in the late quaternary. *Paleoceanography*, *24*(2). https://doi.org/10.1029/2008PA001659

Sikes, E. L., Samson, C. R., Guilderson, T. P., & Howard, W. R. (2000). Old radiocarbon ages in the southwest Pacific Ocean during the last glacial period and deglaciation. *Nature*, *405*(6786), 555–559. https://doi.org/10.1038/35014581

Skinner, L. C., Fallon, S., Waelbroeck, C., Michel, E., & Barker, S. (2010). Ventilation of the deep Southern Ocean and deglacial CO_2 rise. *Science*, *328*(5982), 1147–1151. https://doi.org/10.1126/science.1183627

Skinner, L. C., Primeau, F., Freeman, E., De La Fuente, M., Goodwin, P. A., Gottschalk, J., et al. (2017). Radiocarbon constraints on the glacial ocean circulation and its impact on atmospheric CO_2. *Nature Communications*, *8*(1), 16010. https://doi.org/10.1038/ncomms16010

Soulet, G. (2015). Methods and codes for reservoir–atmosphere 14 C age offset calculations. Software. *Quaternary Geochronology*, *29*, 97–103. https://doi.org/10.1016/j.quageo.2015.05.023

Talley, L. D., Pickard, G. L., Emery, W. J., & Swift, J. H. (2011). Southern Ocean. In *Descriptive physical oceanography: An introduction*. 6th edition (pp. 437–471). Elsevier Ltd. https://doi.org/10.1016/b978-0-7506-4552-2.10013-7

Thöle, L., Ai, X., Auderset, A., Schmitt, M., Moretti, S., Studer, A., et al. (2022). Migration of the Antarctic polar front over the last glacial cycle (preprint). *Review*. https://doi.org/10.21203/rs.3.rs-1364006/v1

Toggweiler, J. R., Russell, J. L., & Carson, S. R. (2006). Midlatitude westerlies, atmospheric CO_2, and climate change during the ice ages. *Paleoceanography*, *21*(2), PA2005. https://doi.org/10.1029/2005PA001154

Umling, N. E., Sikes, E., Rafter, P., Goodkin, N. F., & Southon, J. R. (2024). The benthic and planktic foraminiferal oxygen isotope and radiocarbon data for article "Deglacial carbon escape from the northern rim of the Southern Ocean" [Dataset]. National Centers for Environmental Information. https://www.ncei.noaa.gov/access/paleo-search/study/39058

WAIS Divide Project Members. (2015). Precise interpolar phasing of abrupt climate change during the last ice age. *Nature*, *520*(7549), 661–665. https://doi.org/10.1038/nature14401

Watanabe, O., Jouzel, J., Johnsen, S., Parrenin, F., Shoji, H., & Yoshida, N. (2003). Homogeneous climate variability across East Antarctica over the past three glacial cycles. *Nature*, *422*(6931), 509–512. https://doi.org/10.1038/nature01525

Yamazaki, K., Aoki, S., Katsumata, K., Hirano, D., & Nakayama, Y. (2021). Multidecadal poleward shift of the southern boundary of the Antarctic circumpolar current off east Antarctica. *Science Advances*, *7*(24), eabf8755. https://doi.org/10.1126/sciadv.abf8755

Zhao, N., Marchal, O., Keigwin, L., Amrhein, D., & Gebbie, G. (2018). A synthesis of deglacial deep-sea radiocarbon records and their (in)consistency with modern ocean ventilation. *Paleoceanography and Paleoclimatology*, *33*(2), 128–151. https://doi.org/10.1002/2017PA003174